Impact of Multi-beam Antenna Amplitude Tapering on Co-Channel Interference and Backhaul Throughput Density

Nizabat Khan[1], Tao Jiang[2], David Grace[2], Alister G. Burr[2], Claude Oestges[1]

[1]ICTEAM, Universite catholique de Louvain (UCL), Louvain la Neuve, Belgium
[2]Department of Electronics, University of York, York, UK
nizabat.khan@uclouvain.be

***Abstract*— Multi-beam antennas, combined with aggressive frequency reuse have recently been considered to increase the throughput density in densely deployed cellular networks. However, the latter is limited by Co-Channel Interference (CCI). To mitigate this problem, amplitude tapering in multi-beam antenna scenarios is investigated in this paper. Results show that tapered beams significantly improve the Carrier to Interference Ratio (CIR) from 5 to 8 dB and consequently achieve downlink backhaul throughput density over 0.6 Gbps/km^2. An overall throughput density of 1.2 Gbps/km^2 is expected when taking both up- and downlinks into account.**

Keywords-component; Amplitude tapering, Co-channel Interference, Throughput density, Multi-beam Antenna

I. INTRODUCTION

The BuNGee (Beyond Next Generation mobile broadband) project aims to dramatically improve the overall capacity density provided by a mobile network to an ambitious goal of 1 Gbps/km^2 in the cell at a commercially viable cost – thereby removing the barrier to beyond next generation networks deployment [1]. The BuNGee innovative architecture combines a number of technological paradigms. It relies on a Hub Base Station (HBS) connected to the operator back-haul on one side and to the distributed Access Base Stations (ABSs) or fixed relays on the other side. To address constantly growing capacity demand, high spectral and spatial reuse combined with high spectrum efficiency is desired. HBS antenna beams allow the spatial reuse of spectrum and thus the spectral efficiency tends to increase as cell sizes are reduced. Aggressive frequency reuse based on dual-polarized multi-beam antennas for terrestrial communications has not been employed previously.

BuNGee utilizes very narrow antenna beams to reduce Co-Channel Interference (CCI) to an acceptable level. However, reducing the beamwidth lower than 15°-20° significantly increases the effective pathloss [2]. For example, using narrow beam of 15° beamwidth causes approximately 9 dB increase in the effective pathloss [2]. Hence a tradeoff between acceptable CCI level and effective pathloss needs to be investigated. This implies that practical beams (15° in BuNGee) still have the potential to interfere with each other, thus not fully removing the CCI. Consequently, CCI causes the main impairment which limits the envisioned throughput density of the backhaul network. The farther the co-channel beams are separated from each other; the lower the expected CCI level as the antenna pattern gradually tapers off with increasing angles from the boresight. However, this gradual taper in the antenna pattern is irregular due to the oscillatory side-lobes. Hence, CCI is a direct consequence of antenna side-lobes and it is evaluated in terms of Carrier Interference Ratio (CIR). For a given scenario, CIR at a particular location can be expressed as,

$$CIR = \frac{P_{max}(ABS)}{\sum_{i=1}^{n} P_i(ABS)} \quad (1)$$

where, $P_{\max}(ABS)$ is the maximum power of a certain beam from a multi-beam HBS antenna at a particular ABS location and is therefore defined as the carrier (the wanted signal). The denominator in (1) is the sum of the powers from all the other interferer HBS beams (same frequency channel) at the same ABS location, regarded as the aggregate interference.

To further reduce the amount of CCI, the use of amplitude tapering (reduced side-lobes) of the antenna beams may be a promising solution [3]. Therefore, the main focus of this paper is to analyze the impact of amplitude tapering in multi-beam antenna on downlink CCI by means of a ray-tracing tool [4-6] and subsequently determine throughput densities through system level simulations. The ray-tracing tool is particularly innovative in that it models not only specular contributions (like all ray-based tools), but also dense multipath (or diffuse scattering) components. These allow to account for macroscopic roughness effects, such as windows, balconies, and surface roughness, etc, which also arise in non-specular directions. Therefore, it provides a much better coverage and interference model than classical tools. Moreover, it has been experimentally validated through the measurement campaign in an outdoor scenario with linear arrays of four dual-polarized ($\pm 45°$ slanted polarizations) antennas [5].

The paper is organized as follows: Section II describes the simulation setup and amplitude tapering. Section III discusses and analyzes the CCI results of three patterns based on ray-tracing simulations in detail. In Section IV, the impact of amplitude tapering on throughput density of the self-backhaul network is analyzed through system level simulations. Finally, conclusions are drawn in Section V.

II. Simulation Setup

A typical urban grid is considered as the test propagation environment for the HBS-to-ABS channel at 3.5 GHz. The deployment square topology [1] has block raster of 90 m, with each block of width 75 m and street width taken as 15 m. Building height is constant and fixed to 20 m. The block diagram explaining the details of scenario is shown in Fig. 1, where HBSs located at the centre of cell utilizes only 12 beams (out of 24 beams in total) for the sake of simplicity. Different colours denote the frequency channels assigned to the HBS beams. Dots show the locations of ABS relay antennas at the street intersections. Arrows show the direction of ABS antennas. Moreover, red dots (ABS18-23) and blue rings (ABS12-17) represent Obstructed Line Of Sight (OLOS) and Non Line Of Sight (NLOS) directions respectively. Both utilized antennas are envisaged and designed by Cobham Antennas specifically for the BuNGee project [7].

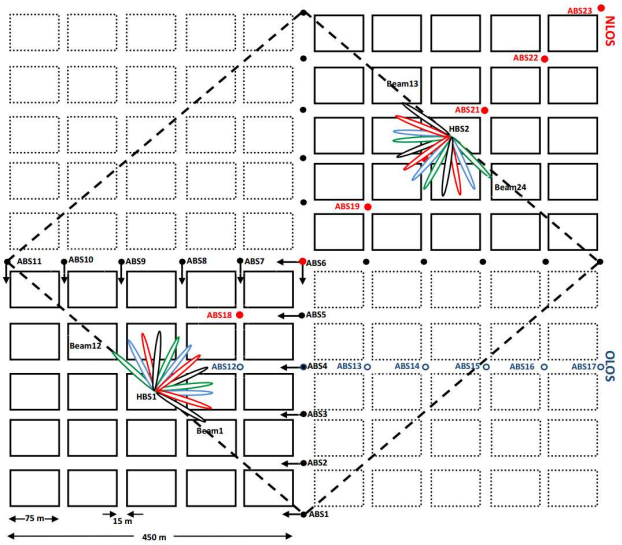

Fig. 1 Manhattan-like grid scenario with square topology

A. HBS Antennas

HBSs are placed in the centre of the blocks at a height of 25 m from the ground level (i.e. 5 m above the rooftop) and equipped with multi-beam directional antennas. Each HBS antenna comprises 4×90° sectors; each sector is capable of providing six separate beams in two slanted ±45° polarizations. The dual-polarization is used to optimize the isolation between adjacent antennas in the array. HBS beams are not intended for specific ABS locations, thus providing choice to select the best available link in the defined architecture. The elevation beamwidth of all beams is approximately 10° with 2° electrical down-tilt [1].

B. Amplitude Tapering

In order to reduce side-lobes (and hence CCI) in azimuth relative to the main beam, amplitude tapering is applied using in-line attenuators between the beam-forming network and the antenna inputs. A beam-forming network connected to the 8-element antenna array produces a unique combination of 6 narrow beams across a 90˚ sector [7]. A bespoke Butler matrix is used in conjunction with 450 mm long phase matched cables to each of antenna input ports. Three patterns of different side-lobes are attained by using combination of low value series attenuators at the eight antenna ports. Two central ports remain un-attenuated (or 0 dB attenuators to preserve the fidelity). The next two ports utilize either 0 dB or 1 dB, while the remaining ports have progressively larger value attenuators such that the greatest attenuation occurs at extremities of the array [7]. Various parameters of the three patterns are summarized in Table I. Beamwidth and peak gains of narrow beams vary slightly with amplitude tapering. Pattern 1 is without amplitude tapering, i.e. normal side-lobes. Pattern 2 (intermediate amplitude tapering) and Pattern 3 (maximum tapering) are illustrated by example beam patterns (azimuth) in Fig. 2 and Fig. 3 respectively. It is worth mentioning that peak gains and beamwidths of narrow beams patterns remain unaffected in the elevation.

C. ABS Antennas

On the ABS (receive) side, directional dual-polarized antennas are used with 13 dBi gain at the height of 5 m from the ground level. Receive antenna has 40° beamwidth both in azimuth and elevation, and two ±45° slanted polarizations. The distance between HBS and ABS antennas varies depending upon the ABS location.

TABLE I. Three Beam Patterns (Azimuth) of HBS Antenna

Parameter		Three side-lobes patterns		
		Pattern 1	***Pattern 2***	***Pattern 3***
Peak Gain [dBi]		18.7	17.2	16.7
Beamwidth [deg]		13.6	14.9	15
1st	Right Sidelobe [dB]	-12.8	-15.6	-17.0
	Left Sidelobe [dB]	-14.3	-17.8	-19.5
2nd	Right Sidelobe [dB]	-15.1	-22.1	-19.3
	Left Sidelobe [dB]	-16.5	-23.8	-20.4
3rd	Right Sidelobe [dB]	-17.4	-21.4	-21.1
	Left Sidelobe [dB]	-27.8	-32.6	-31.6

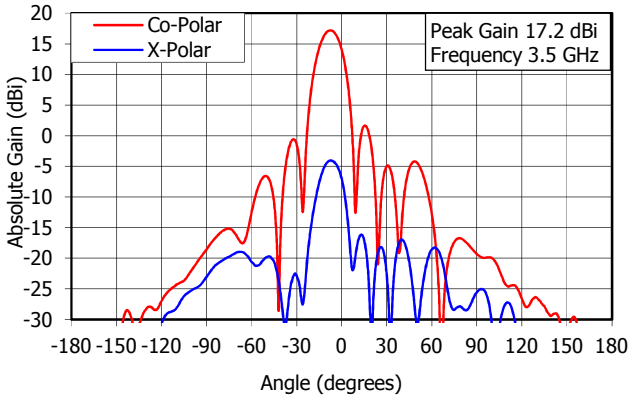

Fig. 2 An example beam pattern (azimuth) of multi-beam HBS antenna with intermediate amplitude tapering (Pattern 2)

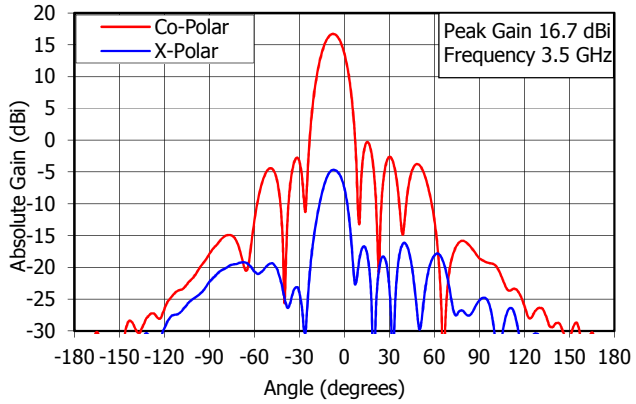

Fig. 3 An example beam pattern (azimuth) of multi-beam HBS antenna with maximum amplitude tapering (Pattern 3)

In the next section, the effects of amplitude tapering (reducing side-lobes without significant degradation of the other characteristics) to suppress the CCI are detailed and analyzed for backhaul HBS-to-ABS links.

III. Analysis of Co-Channel Interference

Consider an HBS cell (as shown in Fig. 1) with N ABSs, and B HBS beams. Frequency reuse in multi-beam HBS antenna is S, thus making B/S number of beams at the same frequency (channel). Each antenna is further divided into R sectors. A desired ABS receives wanted signal P_{max} (largest in magnitude) along with $B/S - 1$ interfering signals, each of them having a power level P_i. Therefore, the aggregate interference I_{agr} can be expressed as,

$$I_{agr} = \sum_{i=1}^{\frac{B}{S}-1} P_i \qquad (2)$$

Naturally, power levels P_i differ at a desired ABS location, due to different HBS beams orientations and multi-paths. Most interfering beams contribute only through side-lobes. However, some of the adjacent interfering beams contribute with the power levels close to P_{max} at the desired ABS, when they have similar arrival paths in the street. CCI in terms of CIR values can be evaluated with the help of (1) and (2).

Moreover, noise is also always present in a real system. Therefore, a certain noise floor level has been taken into account in simulations of backhaul throughput density; however this section is only limited to CIR analysis.

A. Square Topology

Ray-tracing simulations are performed in an interfering environment to demonstrate the advantage of reduced side-lobes. CIR (dB) is evaluated only for the HBS1 cell mentioned in the square topology as shown in Fig. 1. Results of only one frequency band (out of four HBS frequency bands) at each ABS location are presented in Fig. 4. Other frequency bands show similar results. Both amplitude tapered patterns (Pattern 2 and Pattern 3) have significantly improved the performance compared with the non-tapered Pattern 1. CIR improvement ranges from 5 to 10 dB at different ABS locations. However, Pattern 2 performs slightly better than Pattern 3 except at ABS3 and ABS10 locations. This discrepancy might be due to the fact that the 2nd and 3rd side-lobes of Pattern 2 are smaller than those of Pattern 3 (as summarized in Table I), resulting in slightly better performance. Furthermore, the magnitude of the wanted signal (received power) at the desired ABS location remains almost unaffected for three investigated patterns. This fact confirms that the received power or equivalently gain loss is independent of the tapering effect but largely depends upon antenna beamwidths and other relevant channel parameters.

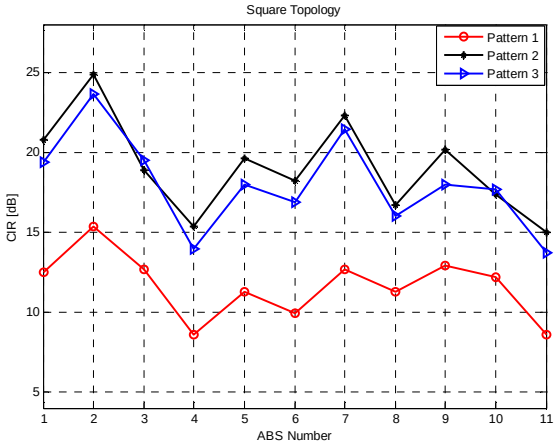

Fig. 4 CIR [dB] for three patterns of HBS antenna beams at ABS locations

B. Obstructed LOS and NLOS Fixed Directions

In Fig. 1, seven ABS antennas are positioned at street inter-sections in two directions:

- OLOS
- NLOS

as depicted by hollow blue and solid red dots respectively. Results illustrated in Fig. 5 follow the ABS nomenclature specified in Table II.

TABLE II. ABS Nomenclature for OLOS and NLOS Directions

Direction	ABS Position	Equivalent ABS Position in Fig. 5
OLOS	12,4,13,14,15,16,17	A,B,C,D,E,F,G
NLOS	18,6,19,20,21,22,23	

Results shown in Fig. 5 confirm again a significant improvement in CIR with amplitude tapered patterns in both directions. However, generally the CIR exhibits better performance in the OLOS than the NLOS direction. CIR improvement is in the range of 5 to 8 dB. It becomes more obvious by this analysis that Pattern 2 performs better than Pattern 3 both in NLOS and OLOS scenarios, again because of the smaller 2nd and 3rd side-lobes of Pattern 2 compared to Pattern 3. It is also worth mentioning that the CIR slightly

increases with the distance along both NLOS and OLOS directions as separation between neighboring HBS beams (at same frequency) increases.

From the above discussion it is evident that amplitude tapering in multi-beam antennas can play an important role in reducing the CCI even in dense deployment scenarios. By controlling the side-lobes of multi-beam antennas, CIR can be maintained above 12dB in an HBS cell which guarantees the required quality of service in BuNGee-like networks. This further ability can lead to increase the backhaul throughput density as described in the next section.

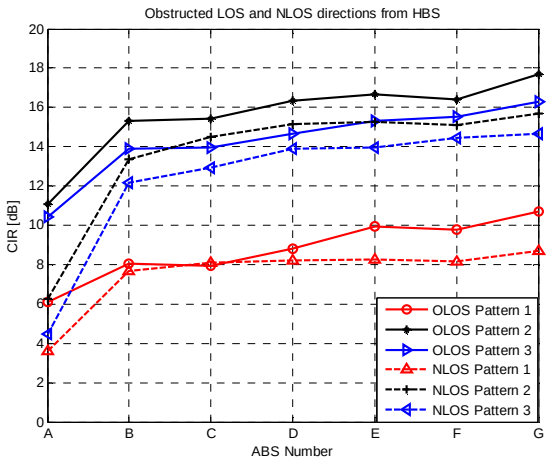

Fig. 5 CIR [dB] for three HBS beam patterns when ABS are placed in OLOS and NLOS directions

IV. BACKHAUL THROUGHPUT DENSITY

The impact of amplitude tapering (thus reduced side-lobes) is investigated at the system level in this section by examining the backhaul throughput density and Grade of Service (GoS) measurements. A Manhattan-grid environment has been used for the system level modeling as shown in Fig. 1. There are 11 streets both East-West (E-W) and North-South (N-S), forming a 10×10-block area. The HBS antennas are placed above rooftop in the centre of the cells and two HBSs cover a 4 cell square deployment environment in this case. The simulated service area is surrounded by the dashed line. Two sectors (12 beams) of each HBS antenna (facing towards the centre area) have been considered. The parameters used are shown in Table III.

TABLE III. PARAMTERS FOR SYSTEM LEVEL SIMULATIONS

Parameter	Value
HBS transmission power	37 dBm
ABS transmission power	27 dBm
Carrier frequency	3.5 GHz
Number of Channels	4
Lognormal shadowing	6 dB
Noise floor	-114 dBm/MHz

The ray-tracing tool is used to estimate the pathloss between the HBS and ABS. The access network (i.e. ABSs to mobile terminals) is assumed to utilize different resources (i.e. time slots or frequency bands) to eliminate potential interferences between the access network and the self-backhaul network. Thus, only the self-backhaul network (i.e. HBS-to-ABS) has been simulated in this paper. The basic Poisson traffic model is applied to generate the traffic. The inter-arrival and service time of transmissions follow the negative exponential distribution.

Four 10 MHz channels for the backhaul network are utilized in the simulation. 30 OFDMA (Orthogonal Frequency Division Multiple Access) format sub-channels are assumed within each 10 MHz channel. At the HBS side, 4 different channels are used for each group of 4 neighboring beams in the order from channel 1 to channel 4. ABSs located at the top and bottom of the cell are designed to serve N-S streets, and ABSs on the left and right serve the E-W streets. The two ABS beams pointing in opposite directions should use two different channels. ABSs that serve N-S streets use two different channels from those that serve E-W streets.

Throughput density is the main measurement used in this paper to describe the performance of backhaul network. The average throughput density can be defined as [8]:

$$Thr_D = Thr_s / A_s \tag{3}$$

where A_s is the service area and Thr_s is the backhaul throughput which can be defined as:

$$Thr_s = \sum_{i=1}^{N_u} \sum_{k=1}^{n_i} \sum_{t=0}^{T_k} Thr_{link}(t) \tag{4}$$

where $Thr_{link}(t)$ is the throughput value of a link obtained at time t, and it is updated constantly in the simulation. T_k is the transmission time of the k^{th} transmission of an entity, and n_i is the total number of transmissions that have been completed by the i^{th} entity in the simulation. N_u is the total number of entities in the simulation [8].

Fig. 6 shows the downlink throughput density performance of the self-backhaul network at different system offered traffic levels. Pattern 2 and Pattern 3 perform better than Pattern 1 due to the reduced side-lobes. Pattern 1 achieves the lowest throughput density, and comparing with Pattern 2 and Pattern 3, the decrease of the performance keeps increasing when the offered traffic level increases. The performance of Pattern 2 and Pattern 3 are identical throughout the simulation. It can be explained in the same way as explained in Fig. 4, with the difference in the performance being only marginal.

Fig. 7 illustrates the GoS measurements of the self-backhaul network. It can be clearly seen that Pattern 1 which has normal side-lobes without amplitude tapering suffers a higher level of interference which in turn leads to a higher level of interruption to the network. Both the blocking probability and dropping probability of Pattern 1 are significantly higher than those with reduced side-lobe patterns. Pattern 2 performs slightly better than Pattern 3.

It can be seen from the figures that a downlink throughput density over 0.6 Gbps/km^2 can be achieved with a satisfactory GoS performance by reducing the side-lobe level of the HBS antenna beams. An overall throughput density of 1.2 Gbps/km^2 can be expected at the self-backhaul network since a 50%-50% Time Division Duplex (TDD) split between downlink and uplink is assumed. Pattern 1 with normal side-lobes can only achieve about 0.25 Gbps/km^2 downlink throughput density if 5% and 0.5% GoS requirements for blocking probability and dropping probability are applied respectively. The overall self-backhaul throughput density is only about 0.5 Gbps/km^2 in this case. A significant improvement in backhaul throughput density is possible through reducing side-lobe levels of the HBS multi-beam antennas.

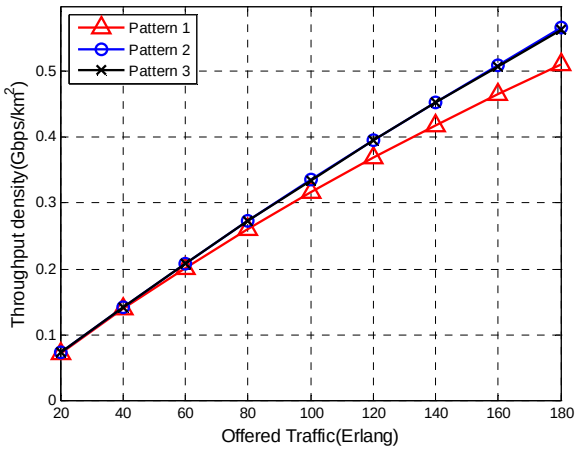

Fig. 6 Downlink throughput density of self-backhaul network

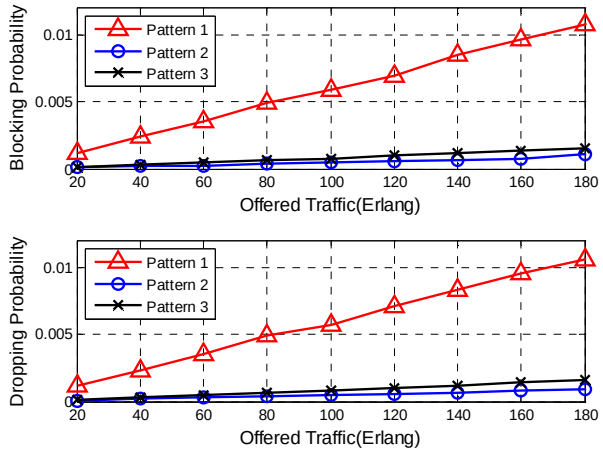

Fig. 7 Self-backhaul network blocking probability and dropping probability

It is clear that the relative gain between the main lobe and side lobes has a significant impact on the self-backhaul network performance, and the relative gain may be better improved in some circumstances by reducing the side lobes rather than boosting the peak gain.

V. CONCLUSIONS

In this paper, the impact of amplitude tapering employed in BuNGee specific innovative multi-beam antenna on CCI and backhaul throughput density has been analyzed. Results have revealed that tapered beams reduce the CCI (improve CIR) significantly, by between 5 and 8 dB. No substantial gain loss has been observed at desired ABS locations, because the peak gains of the investigated patterns are nearly identical. CIR can be maintained above the acceptable level of 12 dB by reducing side-lobes which guarantees the required quality of service in wireless networks. The system level simulations further prove the improvement in backhaul throughput density by amplitude tapering. The mobile broadband system suffers significantly less interruption because of reduced side-lobes which in turn results in a significantly improved achievable backhaul throughput density. The self-backhaul network achieves a downlink throughput density over 0.6 Gbps/km^2. An overall throughput density of 1.2 Gbps/km^2 is expected when taking both up- and downlinks into account. Therefore, amplitude tapering may be a promising solution to suppress the CCI encountered by a multi-beam antenna and hence lead to a higher achievable throughput density.

ACKNOWLEDGMENT

The research leading to these results has received funding from the European Community's Seventh Framework Programme (FP7/2007-2013) under grant agreement no. 248267 (BuNGee). Further, the authors are grateful to Francesco Mani for his help with the ray-tracing tool and Cobham Antennas for the measured antenna data.

REFERENCES

[1] O. Marinchenco, et al, "BuNGee project overview," IEEE International Conference on Microwaves, Communications, Antennas and Electronics Systems (COMCAS), 7-9 Nov, 2011.

[2] N.Khan and C.Oestges, "Impact of transmit antenna beamwidth for fixed relay links using ray-tracing and WINNER II channel models" 5th European Conference on Antennas and Propagation, EuCAP'11, Rome Italy, April 2011.

[3] J. Thornton and D. Grace, "Effect of Antenna Aperture Field on Co-channel Interference, Capacity and Payload Mass in High Altitude Platform Communications," ETRI Journal, vol.26, Oct. 2004.

[4] C. Oestges, *et al.*, "Deterministic channel modeling and performance simulation of microcellular wide-band communication systems," *IEEE Transactions on Vehicular Technology*, vol.51, Nov 2002.

[5] E. M. Vitucci, *et al.*, "Analysis and modeling of the polarimetric properties of scattering from building walls" *IEEE Transactions on Antennas and Propagation*, (in press), June 2012.

[6] F. Mani and C. Oestges, "Ray-tracing evaluation of diffuse scattering in an outdoor scenario," *5th European Conference on Antennas and Propagation, EuCAP '11*, Rome Italy April 2011.

[7] Cobham Antennas, "Beyond Next Generation mobile broadband: BuNGee", Microwave Journal,Vol.55,No.1, January 2012 [Online] Available: www.microwavejournal.com/articles/print/456

[8] M. Goldhamer, et al., "BuNGee Deliverable D1.2: Baseline BuNGee Architecture," November 2010, Available: http://www.ict-bungee.eu/

[9] P. Kyosti, et al., "WINNER II channel models," European Commission, Deliverable IST-WINNER D1.1.2 version 1.1, Sept. 2007.[Online].Available:http://projects.celticinitiative.org/winner+/ WINNER2-Deliverables/